Theor Chem Account (2008) 120:167–175
DOI 10.1007/s00214-007-0293-7

REGULAR ARTICLE

Effects of conjugation in length and dimension on two-photon properties of fluorene-based chromophores

Kiet A. Nguyen · Paul N. Day · Ruth Pachter

Received: 22 January 2007 / Accepted: 20 March 2007 / Published online: 4 May 2007

Abstract We report calculated two-photon (TPA) absorption spectra based upon results obtained from quadratic response time-dependent density functional theory for fluorene-based donor-π-acceptor molecules. Coulomb attenuated functionals with a long-range exchange contribution are applied to predict TPA excitation energies and cross-sections. Observed spectra are explained, and the effects of conjugation and multibranching on the TPA spectra are discussed.

Keywords Two-photon · Cross-section · Excitation energies · Excited-state · Diphenylaminofluorene · Stilbene

1 Introduction

Large two-photon absorption (TPA) cross-sections of donor–acceptor (DA) chromophores based on the dialkylfluorene core (Fig. 1) [1–11] and other DA chromophores [12,13] (e.g. substituted stilbenes (Fig. 2) [14–16]) make them excellent dyes for potential applications, such as photodynamic therapy, [17] confocal microscopy, [18] fluorescence imaging, [19] and optical memory [20].

Recently, it has been demonstrated that a design of multi-dimensional conjugated DA chromophores (see refs. [12,13] for other examples) based on fluorene, [9,11,21] can significantly increase the observed TPA cross-sections. Using the dipolar system with 2-benzothiazolyl as the π-accepting group (see Fig. 1), the conjugation in the DA model that extends from diphenylamino (designated as AF-240) to triphenylamino (AF-270) groups, can be branched at the amine core to give two quadrupolar (AF-287 and AF-295) and two octupolar (of AF-380 and AF-350) systems. [5,11] A collection of experimental results for these two series in Table 1 reveals the large effects of conjugation length and dimension on TPA spectral properties. Although we have included single-wavelength TPA measurements for completeness, these TPA cross-sections are not sufficient to estimate the enhancement within a series of chromophores due to the differences in spectral shape and location of absorption maxima. However, the spectral locations of these single-wavelength measurements make them useful additions to the full spectra. In addition to the large increase in absorption cross-section (Fig. 3), the TPA spectra of the octupolar chromophores were found to be totally different from their linear spectra. [11] Thus, these TPA spectra might be governed by different selection rules and transitions [11] that are yet to be assigned.

Theoretical studies have been carried out to provide qualitative understanding and spectral predictions for a number chromphores [15,16,22] that are dipolar, quadrupolar and octupolar. The splitting of the first dipolar absorption band into two bands for the quadrupolar and (one degenerate) octupolar were predicted [15,16,22] at different levels of theory. However, the precise location of spectral bands and corresponding intensities for multi-polar systems vary widely depending upon the level of theory and the cou-

Contribution of the Mark S. Gordon 65th Birthday Festschrift Issue.

Electronic supplementary material The online version of this article (doi:10.1007/s00214-007-0293-7) contains supplementary material, which is available to authorized users.

K. A. Nguyen (✉) · P. N. Day · R. Pachter
Materials and Manufacturing Directorate,
Air Force Research Laboratory,
Wright Patterson Air Force Base, OH 45433, USA
e-mail: Kiet.Nguyen@WPAFB.AF.MIL

K. A. Nguyen
UES, Inc, Dayton, USA

P. N. Day
Anteon Corporation, Fairfax, USA

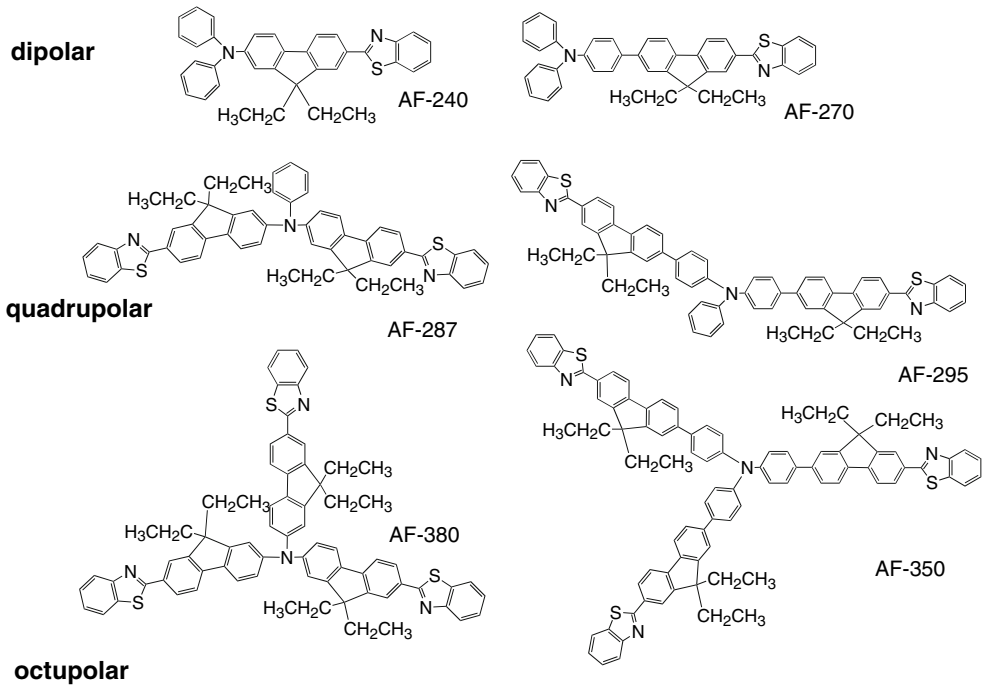

Fig. 1 Structures of substituted fluorene dipolar, quadrupolar and octupolar chromophores

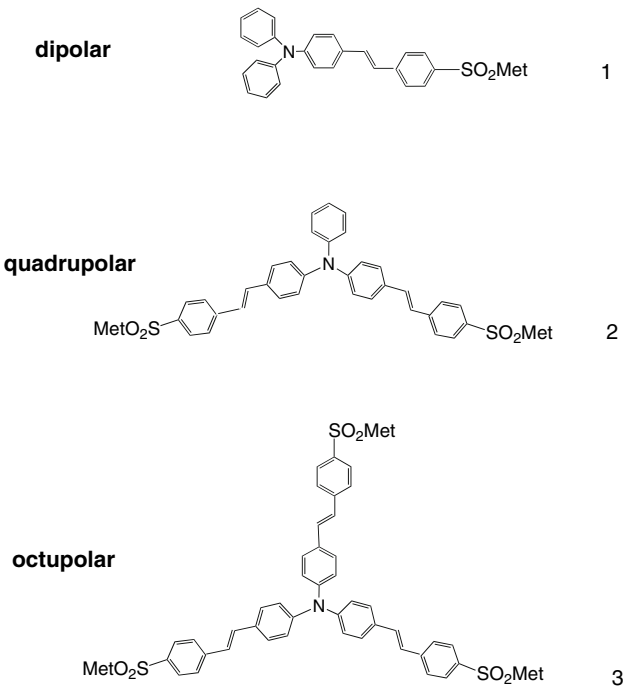

Fig. 2 Structures of substituted stilbene dipolar, quadrupolar, and octupolar chromophores

pling between the branches, which are governed by localized/delocalized nature of excitations involved for a given series of chromophores. We have recently [23] carried out a systematic study of the one-photon absorption (OPA) spectra in the gas-phase and in solvents for a variety of AF chromophores, including the families of chromophores shown in Fig. 1, to assess the quality of the intramolecular charge transfer (ICT) excitation energies and absorption intensities calculated by the widely used Becke's three–parameter hybrid functional (B3LYP), [24–26] the hybrid functional of Adamo and Barone (PBE0), [27] and the CAMB3LYP functional of Yanai et al. [28] The CAMB3LYP functional was based on the solution of the Coulomb-attenuated Schrödinger equation for the local density approximation [29] that was extended to apply to generalized gradient approximation based exchange functionals [30]. CAMB3LYP was constructed by optimizing two parameters ($\alpha = 0.19$ and $\beta = 0.46$) in the long-range-correction for the exchange potential using the G2 database [28]. From the calculated and experimental results, we were able to gauge the relative accuracy of these functionals. PBE0 excitation energies were found to be in better agreement with experiment than B3LYP, with a mean absolute error (MAE) of 0.16 eV for the first ICT bands, which is similar to a MAE of 0.14 eV obtained for dipolar diphenylaminofluorene-based chromophores [31]. On the other hand, we found that CAMB3LYP overestimates the first ICT band of the nine AF chromophores by an average of 0.41 eV. This overestimation of the excitation energies was alleviated by reducing the amount of the long-range exchange contribution to the total energy with a single parameter ($\alpha = \beta = 0.19$). This modification of CAMB3LYP (*m*CAMB3LYP) was found to have a MAE of 0.07 eV for the first ICT energy of diphenylaminofluorene-based chromophores [23].

Table 1 Experimental TPA cross-section (δ, in GM) maxima and corresponding transition energies (in eV)

Molecule/solvent	E (max)	δ (max)	Method	Pulse width (fs)	Reference
AF-240[a]					
THF (fluorescein)	3.02	150	TPF	100	[48]
THF (Coumarin 307)	3.06	135	TPF	100	[48]
Toluene (fluorescein)	3.02	140	TPF	100	[48]
Toluene (Coumarin 307)	3.06	125	TPF	100	[48]
THF (single energy)	3.10	46	Z-scan	105	[21]
AF-270					
THF	3.24	73	WC/Z-scan	140	[11]
THF (single energy)	3.14	50	Z-scan	140	[11]
THF (single energy)	3.10	36	Z-scan	105	[21]
AF-287					
THF (single energy)	3.10	123	Z-scan	105	[21]
AF-295					
THF	3.28	131	WC/Z-scan	140	[11]
THF	3.73	78	WC/Z-scan	140	[11]
THF (single energy)	3.14	50	Z-scan	140	[11]
THF (single energy)	3.10	78	Z-scan	105	[21]
AF-380					
THF	2.98	89	WC/Z-scan	140	[11]
THF	3.38	223	WC/Z-scan	140	[11]
THF (single energy)	3.14	98	Z-scan	140	[11]
THF (single energy)	3.10	157	Z-scan	105	[21]
AF-350					
THF (fluorescein)	3.02	455	TPF	100	[48]
THF (fluorescein)	$\geq$3.47	1035	TPF	100	[48]
THF (Coumarin 307)	3.06	430	TPF	100	[48]
THF (Coumarin 307)	$\geq$3.47	655	TPF	100	[48]
Toluene (fluorescein)	3.02	310	TPF	100	[48]
Toluene (fluorescein)	$\geq$3.47	840	TPF	100	[48]
Toluene (Coumarin 307)	3.06	310	TPF	100	[48]
Toluene (Coumarin 307)	$\geq$3.47	540	TPF	100	[48]
THF (single energy)	3.12	152	Z-scan	135	[5]
THF	3.24	208	WC/Z-scan	140	[11]
THF	3.02	120	WC/Z-scan	140	[11]
THF (single energy)	3.14	133	Z-scan	140	[11]
THF (single energy)	3.10	121	Z-scan	105	[21]

[a] TPA maxima and cross-sections for decyl analog (AF-69): (1) 3.18 eV, 100 GM (Z-scan experiment [10] in THF). (2) 3.22 eV, 72 GM (Fl experiment [51] in hexane). (3) 3.20 eV, 120 GM (WC experiment [10] in THF)

In this study, we focus our attention on the application of quadratic response in time-dependent density functional theory (TDDFT) to address outstanding questions concerning the origins and effects of multidimensional conjugation in the observed TPA spectra of the fluorene-based families of chromophores. Theoretically, the TPA spectra of these fluorene-based chromophores are presently uncharacterized, except for AF-240 [31–33]. To provide additional comparison/evaluation of the theoretical predictions, TPA calculations for a stilbene-based series of chromophores (Fig. 2) [16] that have been experimentally and theoretically characterized are also carried out.

2 Computational methods

2.1 Electronic structure

The TDDFT calculations were carried out at the previously reported B3LYP/6-31G(d) structures [23] using the same

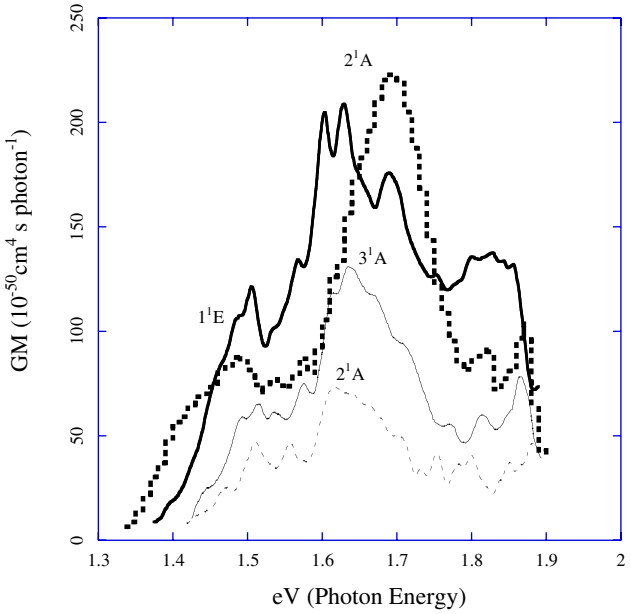

Fig. 3 Experimental [11] TPA spectra for AF-270 (*dashed*), AF-295 (*solid*), AF-350 (*bold*) and AF-380 (*dashed-bold*) in THF

basis set as those used in the ground–state DFT calculations, since the basis set effects were previously [23] found to be small. To gauge the effects of solvent on the TPA cross-sections, we applied the nonequilibrium continuum self-consistent reaction field (SCRF) model of Mikkelsen et al. [34] In the SCRF model, the solute is placed in a spherical cavity with the radii (a_0) obtained from the largest interatomic distances of the solutes with added adjustments for van der Waals interactions. All electronic structure calculations were carried out using the Dalton program [35].

2.2 Two-photon cross-section

The TPA cross-section can be obtained by relating the absorption rate [31,36–38] to the TPA transition probability, which was first derived by Goppert-Mayer [39] using second-order perturbation theory [40]. Using the normalized Gaussian line shape function, [31,41] the two-photon absorptivity can be written as

$$\delta(2E_\lambda) = \frac{16\pi^4}{c^2 h}\left(\frac{\ln 2}{\pi}\right)^{1/2} E_\lambda^2 \sum_f \frac{|S_{f0}|^2}{E_f^{\mathrm{FWHM}}} \times \exp\left[\frac{-4\ln 2}{(E_f^{\mathrm{FWHM}})^2}\left(2E_\lambda - E_f\right)^2\right], \quad (1)$$

where c is the speed of light, h Planck's constant, E_λ photon energy, S_{f0} the TPA matrix element for a two-photon transition between the ground- (0) and exited-state f. In this study, the TPA matrix elements were computed using the single-residue (SRQR) quadratic response [42–44] method for linearly polarized photons with parallel polarization that are averaged over all orientations of the molecule [45–47]. In addition, the TPA matrix elements were also computed using the sum-over-state (SOS) method with DFT ground state dipoles, transition dipoles and excitation energies from linear response TDDFT, and excited dipoles and excited-to-excited transition dipoles from the double-residue (DRQR) quadratic response function [42–44]. The DRQR-SOS method is computationally more demanding, but offers insights into the mechanism of TPA. However, the DRQR-SOS cross-sections for the AF chromophores (Fig. 1) were not converged to the corresponding SRQR results with the lowest five excited states in the SOS sum due to the importance of contributions of higher excited states. The full-width at half-maximum (FWHM, E_f^{FWHM}) of 0.37 eV, obtained from the experimental TPA spectrum AF-240 in THF, [48] was used in the cross-section calculations for AF-240, AF-287 and AF-380. For AF-270, AF-287 and AF-350, a FWHM of 0.44 eV, obtained from the experimental TPA spectrum AF-270 in THF, [11] was used. As previously noted, [31] the peak TPA cross-section computed using a Gaussian lineshape function is a factor 1.48 larger than that obtained with a Lorentzian, and a different definition of the degenerate TPA rate leads to TPA cross-sections twice [32,40,47] that of Eq. 1.

3 Results and discussion

The TPA experimental results of maximum cross-section corresponding energy are organized in Table 1 while the calculated results are tabulated in Table 2. Table 1 also includes single-wavelength TPA measurements, which are useful in some cases where the spectral locations of these measurements were made near the absorption maxima. Table 2 lists the computed excitation energies, cross-section for each electronic state, as well as the peak energies and cross-sections from the sum of Gaussians that can be directly compared to the corresponding experimental values in Table 1. These experimental values were obtained by digitization of the cited absorption spectra. Overall, we found that qualitative comparisons are not affected by the functionals used. For the DA chromophores based on dialkylfluorenes, PBE0 (CAMB3LYP) underestimates (overestimates) the excitation energies while *m*CAMB3LYP predicts more accurate energies (see Supporting Information). Thus, *m*CAMB3LYP results are used for discussion throughout, unless noted otherwise. We begin with the TPA spectrum of AF-240, then discuss the effects of the phenyl groups and multi-branching. The one-electron excitation origins of these transitions and their properties, which have been discussed previously, [23] will not be repeated here. In light of experimental attempts [49] to correlate the CT character of excited states to their TPA cross-sections, it is worthwhile to note that

Table 2 Calculated SRQR/6-31G(d) TPA energies (in eV) and cross-sections (δ, in GM, using Gaussian lineshape). The maximum energy and cross-section obtained from Eq. 1 are in parentheses

Functional/ state				
	AF-240		AF-270	
	E	δ^a	E	δ^b
*m*CAMB3LYP				
2^1A	3.22 (3.24)	152 (153)[c]	3.29 (3.32)	215 (219)[d]
3^1A	4.03	0	3.86	272
4^1A	4.11 (4.15)	291 (331)	4.10	0
5^1A	4.25	16	4.15 (4.10)	415 (530)
6^1A	4.35	74	4.28	13
SCRF-*m*CAMB3LYP				
2^1A	3.20 (3.22)	172 (173)	3.25 (3.29)	235 (239)
3^1A	4.02	0	3.84	350
4^1A	4.09 (4.11)	388 (409)	4.10	1
5^1A	4.24	19	4.14 (4.09)	549 (690)
6^1A	4.33	23	4.27	15
	AF-287		AF-295	
	E	δ^a	E	δ^b
*m*CAMB3LYP				
2^1A	3.04	61	3.17	84
3^1A	3.35 (3.37)	613 (625)	3.38 (3.47)	629 (756)
4^1A	3.94	25	3.81 (3.81)	749 (920)
5^1A	3.97 (4.00)	812 (949)	3.81	109
6^1A	4.05	122	4.05	6
	AF-380		AF-350	
	E	δ^a	E	δ^b
*m*CAMB3LYP				
1^1E	3.02	129	3.17	153
2^1A	3.50 (3.52)	1393 (1422)	3.46 (3.48)	1127 (1316)
2^1E	3.88	11	3.78	192
3^1A	3.94 (3.95)	1096 (1136)	3.78	193

[a] Using FWHM of 0.37 for AF-240, AF-287, and AF-380
[b] Using FWHM of 0.44 for AF-270, AF-295, and AF-350
[c] DRQR-SOS cross-sections using a two- (δ_{2S}) and five-state (δ_{5S}) approximations: $\delta_{2S} = 332$ GM, $\delta_{5S} = 217$ GM
[d] DRQR-SOS cross-sections using a two- (δ_{2S}) and five-state (δ_{5S}) approximations: $\delta_{2S} = 690$ GM, $\delta_{5S} = 233$ GM

TPA arises from the interactions from *all* individual states and thus to be examined. The DRQR-SOS cross-sections obtained with a small number of states, especially a two-state approximation, were found to have large discrepancies (Table 2) with the corresponding cross-sections analytically evaluated from SRQR method, even for dipolar AF systems.

3.1 AF-240 and AF-270

The first excited state of AF-240 exhibits strong TPA by simultaneously absorbing two photons, each having half of the excitation energy. Experimentally, TPA maxima of AF-240 [48] and its decyl derivative (AF-69) [10,50] are reported to occur at about 3.0–3.2 eV (see Table 1) [10,51]. However, the observed peak cross-sections vary widely, 72–150 GM. TPA in these dipolar systems have been found to originate from the first strongly allowed one-photon state with large changes in the dipole moment between the ground and the final state, using the so-called two-state approximation [31,32] and quadratic response methods [33,52]. The CAMB3LYP/6-31G(d)//B3LYP/6-31G result reported by Rudberg et al. [33] for the first excitation energy (2.58 eV) of AF-240 is about the same as our CAMB3LYP/6-31G(d)//

B3LYP/6-31G(d) value. As noted previously, CAMB3LYP overestimates the first excitation energy of AF-240 [23] and AF-69 [52] by a significant amount, even after accounting for the effects of basis set and solvents. The *m*CAMB3LYP energy of 3.22 eV (3.21 eV in THF) and TPA cross-section of 112 GM (120 GM in THF) for AF-69 were found to be in better agreement with experiment [52]. Not surprisingly, the effects of solvent on the energy and cross-section were also found to be small for AF-240 (see Table 2). The calculated AF-240 cross-sections are slightly larger due to the smaller FWHM used in the calculations. The predicted cross-section of 173 GM is in good agreement with the two-photon fluorescence (TPF) values (cf. Tables 1, 2).

The dipolar arrangement of AF-270, adding a phenyl ring to AF-240, induces slight changes in color (0.05 eV blueshift in THF) and intensity (~60 GM), as predicted by TDDFT. Comparing the TPF (AF-240) and WC/Z-scan (AF-270) values also indicates a blueshift. However, given the large discrepancies in the TPA cross-sections found between the TPF and WC/Z-scan experiments, it is unclear whether they can be independently used to study the structure–property relationship. Although the predicted maximum (3.29 eV) is in good agreement with the experimental maximum (3.24 eV), the computed maximum cross-section of 219 GM, is much larger than the experimental value of 73 GM [11].

3.2 AF-287 and AF-295

The TPA spectrum of AF-287 has not been reported. A TPA cross-section measurement at 3.10 eV (800 nm) was reported [21] to be 123 GM, which is 77 GM (a factor of 2.2) larger than the value obtained for AF240. Interestingly, the corresponding measured cross-section for AF-295 of 78 GM is significantly smaller, which resulted in an increase of 42 GM relative to AF-270 [21]. The increase in TPA intensity upon going from the dipolar AF-270 to quadrupolar AF-295 is consistent with WC/Z-scan spectra, which show an enhancement (1.8) of about 60 GM at peak intensity (Fig. 3). The double branching of AF270 also produces a slight blue-shift of 0.04 eV for the maximum (see Table 1 and Figure 3). This is smaller than the computed blue-shift of 0.15 eV, which is attributed to the more intense and higher energy of the 3^1A state that largely underlies the first TPA band of AF-295. This band has a shoulder at about 3 eV, which may be assigned to the first (2^1A) excited state. The experimental TPA enhancement factor of 1.8 is also smaller than the predicted value of 3.5 for the first band, which is predicted to have a peak cross-section of about 750 GM. TDDFT also predicts another peak at 3.81 eV with a slightly larger cross-section, which is consistent with the maximum observed at 3.73 eV. The corresponding observed intensity (78 GM), however, is much smaller than the first band and that of the predicted value.

3.3 AF-380 and AF-350

The octupolar designs of AF-380 and AF-350 are based on the triphenylamine core but with three identical branches derived from AF-240 and AF-270, respectively. Experimentally, the TPF spectra of AF-350 [48] reveal the first TPA maximum at 3.02 eV with cross-sections in the range of 310–455 GM, while the second maximum was estimated to occur at $\geq$ 3.47 eV with cross-sections in the range of 540–1,035 GM. In contrast, the WC/Z-scan spectrum [11] in THF has a progression that appears to peak at 3.24 eV with a cross-section of about 208 GM. In addition, two less intense features (Fig. 3) at the low and high energy sides that correspond to transition energies of 3.01 eV (121 GM) and 3.38 eV (176 GM) were observed. The first calculated transition (1^1E) at 3.17 eV with the total predicted cross-sections of 306 GM is in reasonable agreement with the TPF results but larger ($2.5x$) than the WC/Z-scan value. The next transition (2^1A) at 3.47 eV is predicted to have a much larger cross-section (1,127 GM) which may be assigned to the second band in the TPF spectra [48].

From the reported [11] WC/Z-scan TPA spectrum in THF, AF-380 is found to have more clearly identified maxima at 1.49 eV (89 GM) and 1.69 eV (223 GM) that correspond to the respective transition energies of 2.98 and 3.38 eV, which may be correlated with the 1^1E (3.02 eV) and 2^1A (3.50 eV) excited states, respectively. The first 1^1E excited state has a total predicted cross-section of 258 GM but appears as a shoulder due to a strong overlap with a more intense (1,393 GM) 2^1A state. The cross-sections of these two transitions are much larger than the WC/Z-scan values. However, given the uncertainty in the computed lineshape, the computed 1^1E cross-section is in reasonable agreement with the Z-scan cross-section of 157 GM at 3.10 eV, [21] which is a factor of 1.8 larger than the WC/Z-scan value.

3.4 Comparison with substituted stilbene chromophores

To provide a direct comparison to the dipolar (**1**), quadrupolar (**2**) and octupolar (**3**) substituted stilbenes (Fig. 2), their TPA spectra are computed at the same level of theory (SRQR-*m*CAMB3LYP/6-31G(d)//B3LYP/6-31G(d)). The results are shown in Table 3 and Fig. 4. Note that the B3LYP/6-31G(d) structure of stilbene has been shown [53] to be in good agreement with this experiment, including the central C=C bond that was resolved to be 1.35–1.36 Å [54]. The experimental and calculated TPA spectra of these substituted stilbenes have been reported previously [16]. The results also provide additional data for the evaluation/confirmation of the present theoretical predictions. The dipolar stilbene **1** is predicted to have a maximum cross-section of 125 GM at 3.20 eV (see Table 3 and Fig. 4), in good agreement with experiment

Table 3 Calculated SRQR-*m*CAMB3LYP/6-31G(d) TPA energy (in eV) and cross-section (δ, in GM, using Gaussian lineshape) for substituted stilbenes compared with experimental results. The maximum energy and cross-section obtained from Eq. 1 are in parentheses

Molecule/state	Theory[a]		Experiment[b]	
	E	δ	E (max)	δ (max)
1				
2^1A	3.20 (3.23)	124 (125)	3.22	90
3^1A	4.09	3		
4^1A	4.28	14		
5^1A	4.37	274		
6^1A	4.56 (4.55)	195 (447)		
7^1A	4.58	62		
8^1A	4.61	268		
9^1A	4.72	48		
10^1A	5.06	4		
11^1A	5.14	2		
2				
2^1A	3.00	75	3.04	195
3^1A	3.40 (3.43)	617 (622)	3.35	420
4^1A	4.04	29		
5^1A	4.12	626		
6^1A	4.30 (4.29)	70 (1032)		
7^1A	4.41	534		
8^1A	4.50	93		
9^1A	4.60	13		
10^1A	4.61	16		
11^1A	4.62	7		
3				
1^1E	3.00 (3.02)	134 (270)	3.04	290
2^1A	3.60 (3.62)	1954 (1974)	>3.52	>995
3^1A	3.99	189		
2^1E	4.11 (4.12)	406 (1386)		
3^1A	4.15	439		
4^1A	4.33	1		
2^1E	4.47	15		

[a] Experimental FWHM values were used: **1**, 0.49 eV for all states; **2**, 0.28 eV for the first excited states, 0.46 eV for other states; **3**, 0.36 eV for all states

[b] TPF experiment (with octylsulfonyl analogs) in toluene. [16]

(3.22 eV and 90 GM) and the previous [16] computed values ($\sim$ 150 GM at 3.10 eV). The observed TPA intensity for **1** is somewhat larger than the 73 GM maximum at 3.24 eV obtained for AF-270 (cf. Tables 1, 3). The predicted transition energies and cross-sections for **2** are similar to corresponding values of AF-287 and AF-295. The first transition for **2** is predicted to occur at 3.0 eV with a cross-section of 75 GM but appears (Fig. 4) as a shoulder due to a strong overlap with a next intense band located at 3.40 eV (622 GM), which is assigned to the 3^1A state. The predicted transition energies are in good agreement with experiment (see Table 3) while the corresponding cross-sections are overestimated [16]. The calculated TPA spectrum for **3** is also in good agreement with the previous predicted and observed spectrum in the low (1^1E) and higher (3^1A) energy regions. The predicted maximum TPA energy (cross-section) of 3.02 eV (270 GM) compares well with the observed value of 3.04 eV (290 GM). However, the predicted increase (by a factor of 2.2) for the first peak cross-section upon going from **1** to **3** is significantly smaller than the corresponding observed increase (a factor of 3.2) due to the overestimation in the dipolar system.

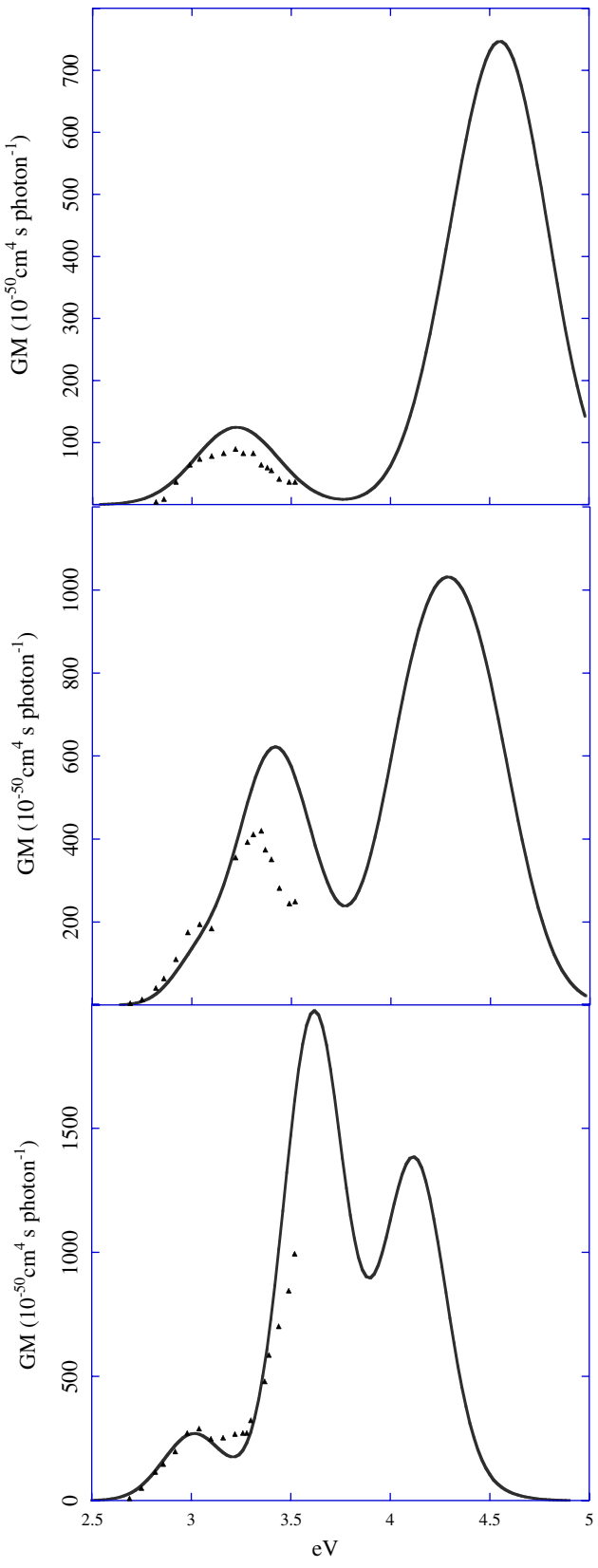

Fig. 4 Experimental (*solid triangle*) [16] and computed (*solid line*) TPA spectra for substituted stilbene **1** (*top*), **2** (*middle*), **3** (*bottom*)

4 Summary and conclusions

In summary, the TPA spectra of the dipolar stilbene **1**, AF-270, and AF-240 are similar but differ markedly from that of their quadrupolar (i.e., **2**, AF-287, AF-295) and octupolar (i.e., **3**, AF-350, AF-380) derivatives due to the differences in the transitions that underlie their absorption spectra. The order of excitation energies of their first absorption bands is dipolar $>$ quadrupolar $\geq$ octupolar. The same ordering of TPA color was experimentally observed. The observed TPA band shifts are attributed to different transitions that underlie the resulting spectra. The first TPA bands in the dipolar systems originate from S_1, while S_1 and S_2 excited states underlie the band in the quadrupolar systems. TDDFT also predicts two transitions (1^1E and 2^1A) which underlie the lowest energy bands that can be assigned to two absorption peaks that are well-resolved in the two-photon WC/Z-scan (AF-380) and fluorescence spectra (**3** and AF-350).

Although our theoretical values are generally well correlated with experiment, there are some large deviations in the cross-sections. Quantitative comparison with experimental TPA cross-sections was found to be complicated by the line-shape functions and the large experimental discrepancies for the AF chromophores. However, good agreement is observed for some AF and substituted stilbene chromophores.

Acknowledgements This research has been supported by the Air Force Office of Scientific Research and by CPU time from the Aeronautical Systems Center Major Shared Resource Center. We gratefully acknowledge a copy of the Dalton program with the CAMB3LYP functional from Prof. Hans Agren.

References

1. Reinhardt BA, Brott LB, Clarson SJ, Dillard AG, Bhatt JC, Kannan R, Yuan L, He GS, Prasad PN (1998) Chem Mater 10:1863
2. Baur JW, Alexander MDJr, Banach M, Denny L, Reinhardt BA, Vaia RA, Fleitz PA, Kirkpatrick SM (1999) Chem Mater 11:2899
3. Belfield KD, Hagan DJ, Van Stryland EW, Schafer KJ, Negres RA (1999) Org Lett 1:1575
4. Belfield KD, Schafer KJ, Liu Y, Liu J, Ren X, Van Stryland EW (2000) J Phys Org Chem 13:837
5. He GS, Swiatkiewicz J, Jiang Y, Prasad PN, Reinhardt BA, Tan L-S, Kannan R (2000) J Phys Chem A 104:4810
6. Kannan R, He GS, Yuan L, Xu F, Prasad PN, Dombroskie AG, Reinhardt BA, Baur JW, Vaia RA, Tan L-S (2001) Chem Mater 13:1896
7. He GS, Lin T-C, Prasad PN, Kannan R, Vaia RA, Tan L-S (2002) J Phys Chem B 106:11081
8. Mongin O, Porrès L, Katan C, Pons T, Mertz J, Blanchard-Desce M (2003) Tetrahedron Lett 44:8121
9. Kannan R, He GS, Lin T-C, Prasad PN, Vaia RA, Tan L-S (2004) Chem Mater 16:185
10. Schafer KJ, Hales JM, Balu M, Belfield KD, Van Stryland EW, Hagan DJ (2004) J Photochem Photobiol A 162:497
11. He GS, Lin T-C, Dai J, Prasad PN, Kannan R, Dombroskie AG, Vaia RA, Tan L-S (2004) J Chem Phys 120:5275

12. Goodson TG III (2005) Acc Chem Res 38:99
13. Goodson TG III (2005) Annu Rev Phys Chem 56:581
14. Chung S-J, Kim K-S, Lin T-C, He GS, Swiatkiewicz J, Prasad PN (1999) J Phys Chem A 103:10741
15. Macak P, Luo Y, Norman P, Agren H (2000) J Chem Phys 113:7055
16. Katan C, Terenziani F, Mongin O, Werts MHV, Porrès L, Pons T, Mertz J, Tretiak S, Blanchard-Desce M (2005) J Chem Phys A 109:3024
17. Spangler CW, Starkey JR, Meng F, Gong A, Drobizhev M, Rebane A, Moss B (2005) Proc SPIE: Int Soc Opt Eng 5689:141
18. Denk W, Strickler JH, Webb WW (1990) Science 248:73
19. Schafer-Hales KJ, Belfield KD, Yao S, Frederiksen PK, Hales JM, Kolattukudy PE (2005) J Biomed Opt 10:051402
20. Kirkpatrick SM, Baur JW, Clark CM, Denny LR, Tomlin DW, Reinhardt BR, Kannan R, Stone MO (1999) Appl Phys A 69:461
21. Rogers JE, Slagle JE, McLean AD, Sutherland RL, Brant MC, Heirichs J, Jakubiak R, Kannan R, Tan L-S, Fleitz PA (2006) J Phys Chem A 111:1899
22. Beljonne D, Wenseleers W, Zojer E, Shuai Z, Vogel H, Pons SJK, Perry JW, Marder SR, Bredas J-L (2002) Adv Funct Mater 12:631
23. Nguyen KA, Rogers JE, Slagle JE, Day PN, Kannan R, Tan L-S, Fleitz PA, Pachter R (2006) J Phys Chem A 110:13172
24. Becke AD (1993) J Chem Phys 98:5648
25. Becke AD (1988) Phys Rev A 38:3098
26. Lee C, Yang W, Parr RG (1988) Phys Rev B 37:785
27. Adamo C, Barone V (1999) J Chem Phys 110:6158
28. Yanai T, Tew DP, Handy NC (2004) Chem Phys Lett 393:51
29. Gill PMW, Adamson RD, Pople JA (1996) Mol Phys 88:1005
30. Tawada Y, Tsuneda T, Yanagisawa S, Yanai T, Hirao K (2004) J Chem Phys 120:8425
31. Day PN, Nguyen KA, Pachter R (2005) J Phys Chem B 109:1803
32. Guo J-D, Wang C-K, Luo Y, Agren H (2003) Phys Chem Chem Phys 5:3869
33. Rudberg E, Salek P, Helgaker T, Agren H (2005) J Chem Phys 123:184108
34. Mikkelsen KV, Dalgaard E, Swanstrom P (1987) J Chem Phys 91:3081
35. Dalton, Dalton, a molecular electronic structure program, release 2.0, www.kjemi.uio.no/software/dalton.html (2005)
36. Sutherland RL (1996) Handbook of nonlinear optics. Marcel Dekker, New York
37. He GS, Yuan L, Cheng N, Bhawlkar JD, Prasad PN, Brott LL, Clarson SJ, Reinhardt BA (1997) J Opt Soc Am B 14:1079
38. Rumi M, Ehrlich JE, Heikal AA, Perry JW, Barlow S, Hu Z, McCord-Maughon D, Parker TC, Rockel H, Thayumanavan S, Marder SR, Beljonne D, Bredas J-L (2000) J Am Chem Soc 122:9500
39. Goppert-Mayer M (1931) Ann Phys 9:273
40. Peticolas WL (1967) Ann Rev Phys Chem 18:233
41. Birge RR, Zhang C-F (1990) J Chem Phys 92:7118
42. Olsen J, Jørgensen P (1985) J Chem Phys 82:3235
43. Salek P, Vahtras O, Trygve H, Agren H (2002) J Chem Phys 117:9630
44. Salek P, Vahtras O, Guo J, Luo Y, Helgaker T, Agren H (2003) Chem Phys Lett 374:446
45. Monson PR, McClain WM (1970) J Chem Phys 53:29
46. McClain WM, Harris RA, in Excited states, Lim EC (ed.) Academic, New York, vol 3, pp 1
47. Masthay MB, Findsen LA, Pierce BM, Bocian DF, Lindsey JS, Birge RR (1986) J Chem Phys 84:3901
48. Rumi M, Perry JW, 2002, Private communication
49. Ramakrishna G, Goodson TG III (2007) J Phys Chem A 111:993
50. Belfield KD, Schafer KJ, Mourad W, Reinhardt BA (2000) J Org Chem 65:4475
51. Hales JM, Hagan DJ, Van Stryland EW, Schafer KJ, Morales AR, Belfield KD, Pacher P, Kwon O, Zojer E, Bredas JL (2004) J Chem Phys 121:3152
52. Day PN, Nguyen KA, Pachter R (2006) J Chem Phys 125:094103
53. Gagliardi L, Orlandi G, Molina V, Malmqvist P-Å, Roos B (2002) J Phys Chem A 106:7355
54. Ogawa K, Harada J, Tomoda S (1995) Acta Crystallogr B 51:240